

## Negative-sequence current filter based on inductance coils

Mark Kletsel<sup>1</sup>, Bauyrzhan Mashrapov<sup>1</sup>, Rizagul Mashrapova<sup>1</sup>, Alexandr Kislov<sup>2</sup>

<sup>1</sup>Department of Electric Power Industry, Faculty of Energetics, Toraighyrov University, Pavlodar, Kazakhstan

<sup>2</sup>Department of Electrical Engineering and Automation, Faculty of Energetics, Toraighyrov University, Pavlodar, Kazakhstan

### Article Info

#### Article history:

Received Jun 18, 2024

Revised Aug 19, 2024

Accepted Sep 3, 2024

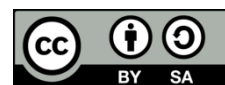
#### Keywords:

Current filter  
Experiment  
Inductance coil  
Negative sequence  
Simulation

### ABSTRACT

The construction of new relay protection systems without the use of current transformers is a fundamental problem of electro energetics, which has not yet been solved. This work suggests a negative-sequence current filter which receives information from inductance coils (ICs) mounted at a safe distance in the magnetic field of phase currents. This filter does not require current transformers, thus saving high-quality copper, steel, and expensive high-voltage insulation in amount unprecedented for relay protection (a 6 to 110 kV current transformer has 19 to 480 kg in weight). A circuit (including functional diagnostics) and a technique for selecting the parameters of filter components and the points where ICs should be fixed are presented; a structure for IC fastening is described. Computer simulation and experiment were used for data collection. The data show that i) the filter conversion coefficient  $m = 1.6$ , and imbalance increases by 7% at the network frequency  $f = 48-52$  Hz; ii) protections based on this filter should have a time delay; iii) the filter is not inferior to well-known well-tested filters with current transformers; and iv) it is functional, but can only be used for single-standing electrical installations.

This is an open access article under the [CC BY-SA](https://creativecommons.org/licenses/by-sa/4.0/) license.



### Corresponding Author:

Bauyrzhan Mashrapov

Department of Electric Power Industry, Faculty of Energetics, Toraighyrov University

16 Tkachev Street, Pavlodar 140000, Kazakhstan

Email: bokamashrapov@mail.ru

## 1. INTRODUCTION

Information about the magnitude of negative sequence currents is commonly used not only in relay protection [1]–[3], but also in electrical installation control devices [4], [5]. In relay protection devices, control of these currents enables increasing sensitivity to asymmetrical operating modes of an electrical installation, including short circuits (SC) [1]. Therefore, protections are designed based on filters [6], which detect these currents, for all generators with of higher than 1,200 MW in power, power transmission lines, and power transformers with of 220 to 750 kV in voltage; these filters are the main components of protections and must be installed [7], [8]. The main disadvantage of such filters, including microprocessor ones, is that they receive information on currents in the phases of an electrical installation from metal-intensive and bulky current transformers (CTs), which introduce additional errors in the magnitude of negative sequence currents, especially when saturated.

Abandonment of CTs remains one of the fundamentally unsolved problems in the electric power industry [9], [10]. This is to provide not only saving in copper, steel, and high-voltage insulation in amounts unprecedented for relay protection technology, but also an increase in electric power system reliability by fully duplicating the relay protection (especially majorization). Today, majorization is extremely seldom used because relay protection CTs are not duplicated due to high cost and bulkiness (a 10 to 110 kV CT weighs 19 to 480 kg). Replacement of CTs with other sensors will require new relay protection devices. Thus,

creation of new relay protections for electric power systems becomes an urgent problem. Attempts to solve it began in the past century. Magnetic current transformers [11], reed switches [12]–[16], Rogowski coils [9], [17]–[23], Hall sensors [24]–[26], and inductance coils (ICs) [27] were suggested to be used as current sensors. The question of which of these sensors is preferable can be answered only after accumulating certain service experience of relay protection devices created on their basis. However, this experience is limited today, as well as the list of such devices.

Thus, negative-sequence current filters without CTs were suggested to design only based on Rogowski coils [28], [29] and reed switches [30], [31]. The former detect negative-sequence currents by controlling the sum of voltages phase shifted in a specified angle using a capacitor and a resistor connected to the outputs of the Rogowski coils which encircle the phase conductors. The latter detect these currents by controlling the total induction of magnetic fields produced by currents in the phases of an electrical installation and acting on a reed switch fixed at a safe distance from them. However, they cannot be used in protections for electrical installations of 330 kV and higher in voltage in most cases. Filters based on Rogowski coils are bulky, since high-voltage insulation is needed to mount Rogowski coils, which makes the weight and size of a current sensor become almost the same as those of a CT. Filters based on reed switches are insufficiently sensitivity, since reed switches have a response threshold, and the further they are from busbars, the higher current is required to trigger them.

In this work, we suggest a negative-sequence current filter without a current transformer based on inductance coils, which, like reed switches, are spaced apart from the phases of an electrical installation to a distance acceptable in terms of safety. Inductance coils have been chosen because they are free of the above listed disadvantages of Rogowski coils and reed switches, do not require stable power supply, have no residual voltage and large spread of parameters like Hall sensors. In addition, they are much smaller and lighter than magnetic current transformers.

## 2. PROPOSED METHOD

### 2.1. Diagram of the suggested filter

Negative-sequence current  $I_2$  filter for electrical installations where the phase bus ducts are located at the vertices of an equilateral triangle consists of two identical duplicating filters F1 and F2 in Figure 1. The duplication increases the reliability of detection of  $I_2$  and enables designing a simple fault diagnosis scheme. Filter F1 (F2) contains as shown in Figure 1: inductance coils (1) and (2) ((3) and (4)) with the same parameters fixed at a safe distance from the bus ducts of phases A, B, and C in their cross-sectional plane  $N_1$  ( $N_2$ ); amplifiers (5) and (6) ((7) and (8)); and phase shifting circuit (PSC) (9) ((10)). Fault detection is performed by comparison circuit (CC) (11).

### 2.2. Principle of design [32]

Let us consider the design of filter F1. The electromotive force (EMF)  $\underline{E}_{\mathcal{F}1}$  at terminals 12 and 13 is proportional to  $I_2$  if the filter parameters and coordinates of ICs 1 and 2 are selected so as (1),

$$\underline{E}_{\mathcal{F}1} = \underline{E}_5 + \underline{E}_9 = K_1 I_2, \quad (1)$$

where  $\underline{E}_5$  and  $\underline{E}_9$  are the EMF at outputs of amplifier 5 and PSC 9;  $K_1$  is the proportionality constant.

Let us represent  $I_2$  from (1) as [33]:

$$3I_2 = (\underline{I}_C - \underline{I}_A) + (\underline{I}_B - \underline{I}_C) \cdot e^{-j120}, \quad (2)$$

where  $\underline{I}_A$ ,  $\underline{I}_B$ , and  $\underline{I}_C$  are the total currents in phases A, B, and C;  $e^{-j120}$  is the complex number which characterizes the counterclockwise phase shift by  $-120^\circ$ . This representation has been chosen with the aim of excluding the effect of magnetic fields produced by residual currents on an IC. When decomposing the phase currents into symmetrical components, these currents compensate each other when subtracting. According to (1) and (2), the following conditions should be evidently met when designing a filter:

$$\underline{E}_5 = K_1(\underline{I}_C - \underline{I}_A); \quad \underline{E}_9 = K_1(\underline{I}_B - \underline{I}_C)e^{-j120}, \quad (3)$$

where

$$\underline{E}_5 = K_{a1}\underline{E}_{IC1}; \quad \underline{E}_9 = K_{a2}\underline{E}_{IC2}e^{j\beta_{PSC}}, \quad (4)$$

$E_{IC1}$  and  $E_{IC2}$  are the EMFs at terminals of ICs 1 and 2;  $\beta_{PSC}$  is the phase shift of PSC 9;  $K_{a1}$  and  $K_{a2}$  are the gains of amplifiers 5 and 6.

The EMFs  $E_{IC1}$  and  $E_{IC2}$  are induced in ICs 1 and 2 by the inductions  $\underline{B}_{IC1}$  and  $\underline{B}_{IC2}$  of the magnetic fields produced by phase currents along the longitudinal axis of the ICs with a phase lag of  $90^\circ$  from  $\underline{B}_{IC1}$  and  $\underline{B}_{IC2}$ , and, as is known from basic electrical engineering, are determined from (5a) and (5b),

$$\underline{E}_{IC1} = 2\pi f W_1 S_1 \underline{B}_{IC1} e^{-j90} = K_2 \underline{B}_{IC1} e^{-j90} \quad (5a)$$

$$\underline{E}_{IC2} = 2\pi f W_1 S_1 \underline{B}_{IC2} e^{-j90} = K_2 \underline{B}_{IC2} e^{-j90}, \quad (5b)$$

where  $W_1$  and  $S_1$  are the number of turns and the cross-sectional area of IC 1 and 2 (their parameters are equal);  $K_2$  is the proportionality constant.

Substituting (5a) and (5b) in (4) and equating (4) and (3), we derive,

$$\underline{B}_{IC1} = \frac{K_1(\underline{I}_C - \underline{I}_A)}{(K_2 K_{a1} e^{-j90})} \quad (6a)$$

$$\underline{B}_{IC2} = \frac{K_1(\underline{I}_B - \underline{I}_C) e^{-j120}}{(K_2 K_{a2} e^{j(\beta_{PSC} - 90)})}. \quad (6b)$$

From (6a) and (6b) shows that to detect  $I_2$  IC 1 (2) should be mounting so as to be affected by the magnetic field produced by currents of only phases A and C (B and C). Let us show how this can be done. Let us define the induction  $B_{IC1}$  using the Biot–Savart law and taking into account the effect of the magnetic fields produced by currents of three phases on IC 1 ( $B_{IC2}$  is defined in the same way):

$$\underline{B}_{IC1} = \underline{B}_{A1} \cos \alpha_{A1} + \underline{B}_{B1} \cos \alpha_{B1} + \underline{B}_{C1} \cos \alpha_{C1} = \frac{\mu_0 \left( \frac{\cos \alpha_{A1}}{l_{A1}} I_{A1} + \frac{\cos \alpha_{B1}}{l_{B1}} I_{B1} + \frac{\cos \alpha_{C1}}{l_{C1}} I_{C1} \right)}{2\pi}, \quad (7)$$

where  $\underline{B}_{A1}$ ,  $\underline{B}_{B1}$ ,  $\underline{B}_{C1}$  are the magnetic inductions at the point of IC 1 induced by currents  $I_{A1}$ ,  $I_{B1}$ ,  $I_{C1}$  in phases A, B, and C;  $\alpha_{A1}$ ,  $\alpha_{B1}$ , and  $\alpha_{C1}$  are the angles between the longitudinal axis of IC 1 and  $\underline{B}_{A1}$ ,  $\underline{B}_{B1}$ , and  $\underline{B}_{C1}$ , respectively;  $\mu_0$  is the permeability of air;  $l_{A1}$ ,  $l_{B1}$ , and  $l_{C1}$  are the distances from the axes of bus ducts of phases A, B, and C to the center of gravity of IC 1.

For  $\underline{B}_{IC1}$  ( $\underline{B}_{IC2}$ ) (7) to be proportional to the difference between the currents of phases A and C (B and C), the following conditions should be met:

$$\frac{\cos \alpha_{C1}}{l_{C1}} = -\frac{\cos \alpha_{A1}}{l_{A1}}; \frac{\cos \alpha_{B1}}{l_{B1}} = 0; \quad (8a)$$

$$\frac{\cos \alpha_{B2}}{l_{B2}} = -\frac{\cos \alpha_{C2}}{l_{C2}}; \frac{\cos \alpha_{A2}}{l_{A2}} = 0. \quad (8b)$$

To fulfill conditions (8), ICs 1 and 2 are mounted in plane  $N_1$  in Figure 1 at a safe distance from the phase bus ducts so as the longitudinal axis of IC 1 coincides with the bisecting line of the angle between the lines connecting the bus ducts of phases A and B and the bus ducts of phases B and C, and the longitudinal axis of IC 2 coincides with the bisecting line of the angle between the lines connecting the bus ducts of phases B and phase A and the bus ducts of phases A and C. The safe distance depends on the voltage class and increases with the voltage, for example, it should be no less than 0.4 m at 35 kV, 1 m at 110 kV, and 2 m at 220 kV. The EMF at the terminals of an IC and, hence, the induced induction in the IC in (5) and (7) decrease inversely proportional to the distance. Experiments and calculations show their values to be of millivolts, and they can be amplified to required values. Hence, the suggested filter will perform its function.

To simplify the calculations, it is convenient to set the centers of gravity of ICs 1 and 2 at points on horizontal line 14 which passes through phase C parallel to line 15 connecting phases A and B in plane  $N_1$ , at distances  $x_1 = -0.5d$  и  $x_2 = 1.5d$  ( $d$  is the distance between conductors of adjacent phases) from point 16 of intersection of the vertical which passes through the bus duct of phase A with line 14, and at angles  $\gamma_1 = 30^\circ$  and  $\gamma_2 = 150^\circ$  between line 14 and the longitudinal axes of ICs 1 and 2. Then,  $l_{A1} = l_{B1} = l_{B2} = l_{C2} = d$ ,  $\alpha_{A1} = \alpha_{C2} = 120^\circ$ ,  $\alpha_{C1} = \alpha_{B2} = 60^\circ$ , and  $\alpha_{B1} = \alpha_{A2} = 90^\circ$ , and from (7) we derive,

$$\underline{B}_{IC1} = \frac{\mu_0}{4\pi d} (\underline{I}_C - \underline{I}_A); \underline{B}_{IC2} = \frac{\mu_0}{4\pi d} (\underline{I}_B - \underline{I}_C), \quad (9)$$

let  $K_{a1}=K_{a2}$ . Then, from (1), (4), (5), and (9), we have (10),

$$\begin{aligned} \underline{E}_{\Sigma 1} &= \frac{\mu_0 K_2 K_{a1}}{4\pi d} (\underline{I}_C - \underline{I}_A) e^{-j90} + \frac{\mu_0 K_2 K_{a1}}{4\pi d} (\underline{I}_B - \underline{I}_C) e^{j(\beta_{PSC}-90)} = \\ &= K_1 [(\underline{I}_C - \underline{I}_A) + (\underline{I}_B - \underline{I}_C) e^{j\beta_{\Phi PC}}]; \end{aligned} \tag{10}$$

From (2) and (10) shows that  $\underline{E}_{\Sigma 1}$  is proportional to  $I_2$  if  $\beta_{PSC}=-120^\circ$ .

Filter  $F_2$  is designed in the same way. Inductance coils 3 and 4 are mounted in plane  $N_2$  relative to the phase bus ducts like ICs 1 and 2 in plane  $N_1$  ( $x_3=x_1, x_4=x_2, \gamma_3=\gamma_1, \gamma_4=\gamma_2$ ). The parameters of amplifiers 7 and 8 and PSC 10 are selected the same as those of amplifiers 5 and 6 and PSC 9. Then,  $\underline{E}_{\Sigma 2}$  at terminals 17 and 18 is proportional to  $I_2$  and equal to  $\underline{E}_{\Sigma 1}$ . The equality  $\underline{E}_{\Sigma 2}=\underline{E}_{\Sigma 1}$  is necessary to perform functional diagnostics of the filter.

### 2.3. Fault diagnostics

Filter faults are detected by comparison circuit 11 in Figure 1, which can be implemented based on a differential amplifier with a relay connected to its output (like in the filter prototype presented below). In this case, EMF  $E_{\Sigma 2}$  and  $E_{\Sigma 1}$  are fed to the inputs of the differential amplifier, and EMF  $\underline{E}_{11} = \underline{E}_{\Sigma 1} - \underline{E}_{\Sigma 2}$  is fed to the relay. Due to errors in mounting the IC and in the parameters of components of filters  $F_1$  and  $F_2$ , this difference is equal to the imbalance EMF  $E_{imb}$  in the absence of faults. If a fault occurs in the circuit of, e.g., IC 3, then  $\underline{E}_{11} > E_{imb}$ , comparison circuit 11 operates and signals about a fault in the filter. The set point  $E_{op}$  of circuit 11 operation is offset from the maximal  $E_{imb}$  in the load mode. This enables identifying faults in the filter before a short circuit (SC) occurs in an electrical installation. However, in this case, circuit 11 operates in the case of this SC even in the absence of faults. For the signal from circuit 11 to not induce incorrect operation of the protection device, it should be blocked in the case where both measuring elements connected to  $F_1$  and  $F_2$  operate. We permit this behavior of the fault diagnostic circuit, since the functionality of the relay protection device is checked after clearing a short circuit.

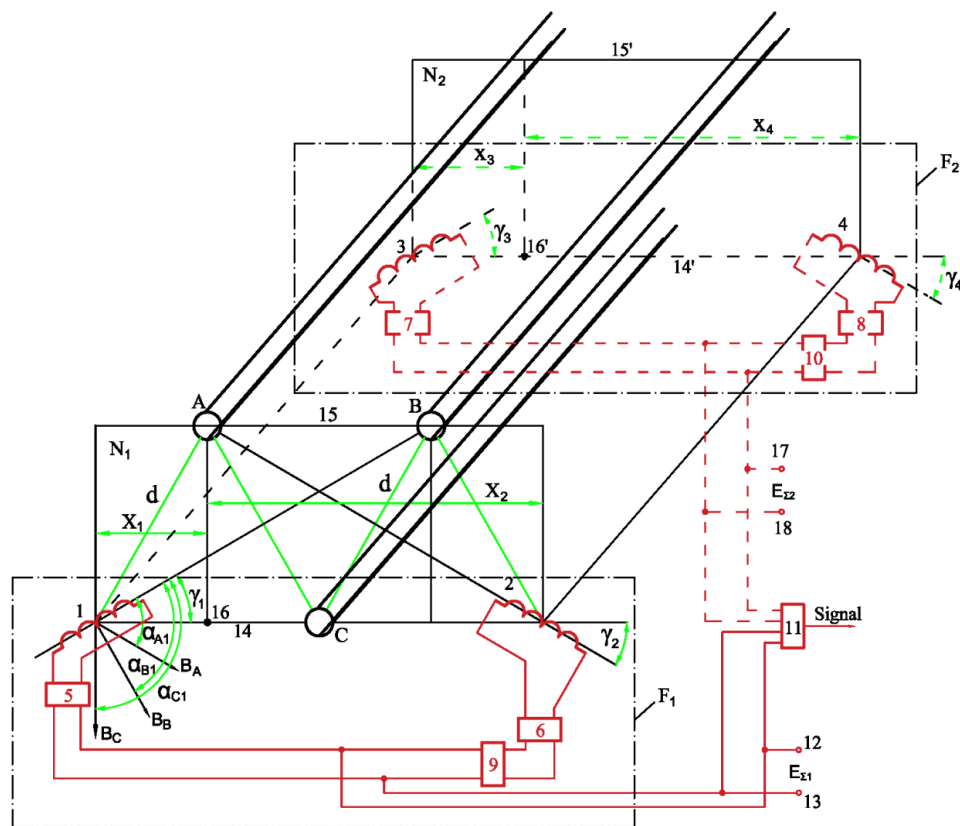


Figure 1. Diagram of the negative-sequence current filter with functional diagnostics

### 3. METHOD

#### 3.1. Computer simulation

To check filter performance, we carried out simulation in MATLAB taking into account the worst effect of errors on  $\underline{E}_{\Sigma 1}$  and  $\underline{E}_{\Sigma 2}$ . A 110-kV one-end transmission line 80 km long in Figure 2 at a load of 30 MW and  $\cos\varphi = 0.95$  was simulated. The distance between the phases was taken to be 1 m (the minimum permissible safe distance). The current in the line phases was measured by current transformers TA1–TA3. Blocks “Goto” and “From” in Figures 2 and 3(a) were used to calculate the magnetic induction. Blocks “Constant,” “Constant1,” “Divide,” and “From” in Figure 3(a) simulated the induction of a magnetic field produced by the current in phase C and affecting IC 1. The inductions of magnetic fields produced by currents in phases A and B and affecting IC 1 in Figure 3(a) are simulated by blocks “Constant4,” “Constant5,” “Divide2,” “From2,” and “Constant2,” “Constant3,” “Divide1,” and “From1” respectively. The values in “Constant,” “Constant2,” and “Constant4” blocks correspond to the ratios  $\frac{\cos\alpha_{C1}}{l_{C1}}$ ,  $\frac{\cos\alpha_{A1}}{l_{A1}}$ , and  $\frac{\cos\alpha_{B1}}{l_{B1}}$  with allowance for mounting errors of 5% towards increasing the distances  $l_{A1}$ ,  $l_{B1}$ , and  $l_{C1}$ ; in blocks “Constant1,” “Constant3,” and “Constant5,” the values correspond to the ratio  $\frac{\mu_0}{2\pi}$ . “Add” block calculates the total induction acting along the longitudinal axis of IC 1. The inductions of magnetic fields affecting IC 3 were simulated in the same way and with the same numerical values in blocks “Constant”–“Constant5”. The inductions of the magnetic fields affecting IC 2 and IC 4 were simulated by replacing the values in blocks “Constant,” “Constant2,” and “Constant4” with  $-0.515$ ,  $0.53$ , and  $-0.017$ , respectively. These values ensure maximal imbalance of the filter. The EMF at the terminals of any of the ICs (with 22,500 turns and a cross-sectional area of  $236 \text{ mm}^2$ ) was simulated using blocks “Constant6”–“Constant8” (where “314” is the product  $2\pi f$ ) and “Divide3” with the same specified numerical values. The filter circuit model is shown in Figure 3(b). Blocks “IC1”–“IC4” are made according to the circuit in Figure 3(a), but with the corresponding coefficients. Blocks “Switch1,” “Switch3,” “Switch4,” “Off Delay1,” “Off Delay3,” “Off Delay,” “Constant1,” “Constant3,” and “Constant4” were used to simulate filter damage at different time points. Blocks “Transport Delay” provide an EMF shift by the angle  $\beta_{\text{PSC}} = -120^\circ$ . Blocks “Switch,” “Switch2,” “Off Delay,” “Off Delay2,” “Constant,” and “Constant2” compensate for the time delay caused by “Transport Delay” blocks. Block “Subtract” simulates a part of comparison circuit 11 in Figure 1) where the difference between voltages  $E_{\Sigma 1}$  and  $E_{\Sigma 2}$  is calculated. Voltages  $\underline{E}_5$ ,  $\underline{E}_9$ ,  $E_{11}$ ,  $\underline{E}_{\Sigma 1}$ , and  $\underline{E}_{\Sigma 2}$  are picked up from outputs 1–5.

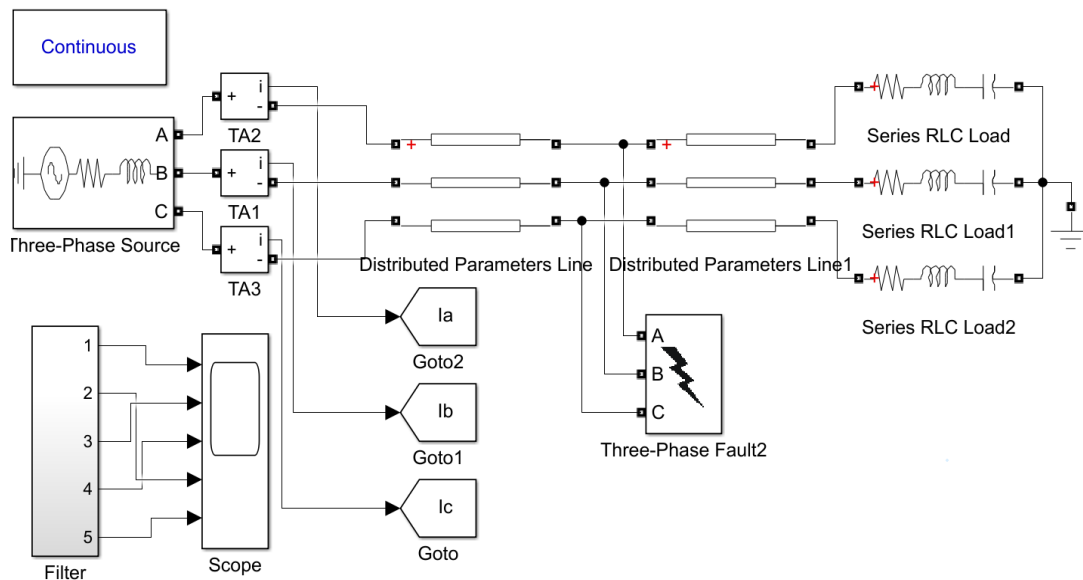


Figure 2. Model of a 110-kv power transmission line

#### 3.2. Filter prototype and experimental setup for its study

Figure 4 shows the laboratory setup: its diagram in Figure 4(a) and assembled setup in Figure 4(b). The laboratory setup includes: load transformer “1” of 35 kVA in power with the transformer ratio 380/2 connected by the primary winding to 380-V electrical network; busbars “2” located at the vertices of an equilateral triangle ( $d=40 \text{ cm}$ ; it is difficult to space them further apart in laboratory conditions); a load in the

form of ballast rheostats “3” (type RB-302, resistance of 0.2 ohm); circuit breaker “4” (type BA57Φ35-340010, rated current of 200 A, and rated voltage of 380 V); DC source “5” (GPC-76030D type, maximal output voltage if 60 V) for powering filter “6”; four-channel oscilloscopes AKIP 4119/2 “7” and AKIP 4119/4 “8” for adjusting the filter. The contacts of breaker 4 on one side are short-circuited to implement two- and three-phase (shown by dashed line in Figure 3) short circuits. Single-phase short circuits cannot be implemented in laboratory conditions. Inductance coils “9–12” (cross section of the IC frame is round; the number of turns is 22,500; the height is 36 mm; the winding thickness is 5 mm, and the inner diameter of the frame is 10 mm including the wall) are mounted exactly like in Figure 1 ( $x_1=-20$  cm and  $x_2=60$  cm,  $\gamma_1=300$  and  $\gamma_2=1,500$ ). Figures 5 shows the laboratory prototype of a negative-sequence current filter: its schematic diagram is shown in Figure 5(a), and the assembled filter is shown in Figure 5(b) (where CC is comparison circuit 11 from Figure 1). The laboratory prototype of filter has been assembled from adjustable R1 (500 kΩ) and R2 (5 kΩ) and non-adjustable R3 (10 kΩ) resistors, operational amplifiers OA (type LM 358), and capacitors C1 (3.3 μF) for demonstrating a possibility of implementing the theoretical calculations.

The experimental procedure is as follows. After assembling the laboratory setup in accordance with the above-described scheme, DC current source “5” and oscilloscopes “7” and “8” are switched on. The source “5” voltage is set to 15 V (operational amplifier voltage). Then, transformer “1” is switched on (breaker “4” is open at this time). The gain factors of voltage amplifiers G1–G4 and the angles of phase-shifting circuits PSC1 and PSC2 are adjusted under the load mode. To do this,  $\underline{E}_{\Sigma 1}$ ,  $\underline{E}_{\Sigma 2}$ , and  $\underline{E}_{11}$  are controlled by oscillograms recorded by oscilloscopes “7” and “8”, and the resistances of resistors R1 and R2 are changed until  $\underline{E}_{\Sigma 1}$ ,  $\underline{E}_{\Sigma 2}$ , and  $\underline{E}_{11}$  become minimum possible. After that, all contacts of breaker “4” on one side as shown in Figure 4(a) are bonded; the breaker is closed, thus producing a three-phase short circuit. Voltage oscillograms are recorded. Breaker “4” is opened. To check the filter operation in the event of a two-phase short circuit, the same operations are repeated, but only two of the three contacts of breaker “4” are bonded. The filter operates as follows under all these modes. The EMFs  $E_{IC1}-E_{IC4}$  from terminals of ICs “9–12” are fed to the entrances of the filter. These EMFs are amplified in amplifiers G1–G4 in Figure 5(a). Voltages from the exits of amplifiers G1 and G3 are fed to some entrances of adders S1 and S2, and from the exits of amplifiers G2 and G4, to other entrances of these adders through phase-shifting circuits PSC1 and PSC2, where they are shifted by  $-120^\circ$ . As a result, adders S1 and S2 output voltages  $\underline{E}_{\Sigma 1}$  and  $\underline{E}_{\Sigma 2}$ , which are fed to the inputs of comparison circuit CC, which outputs voltage  $E_{11}$ .

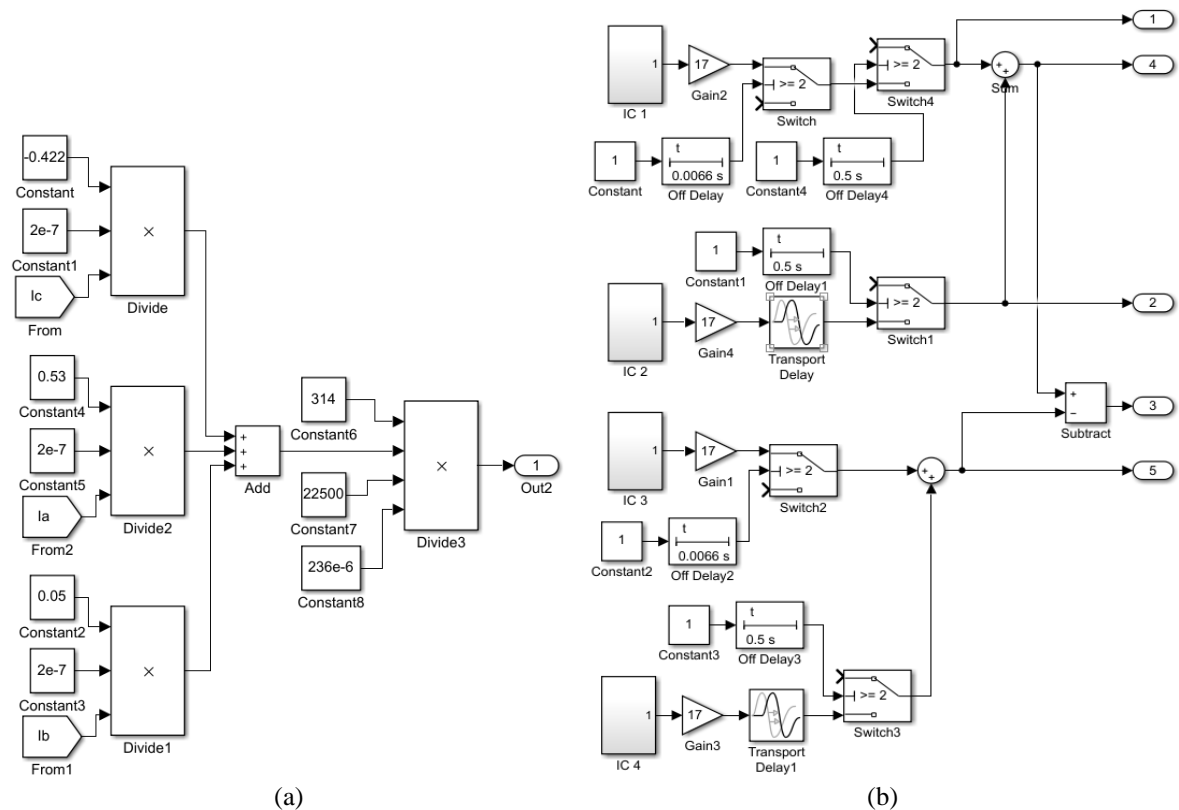


Figure 3. Model of (a) IC and (b) negative-sequence current filter

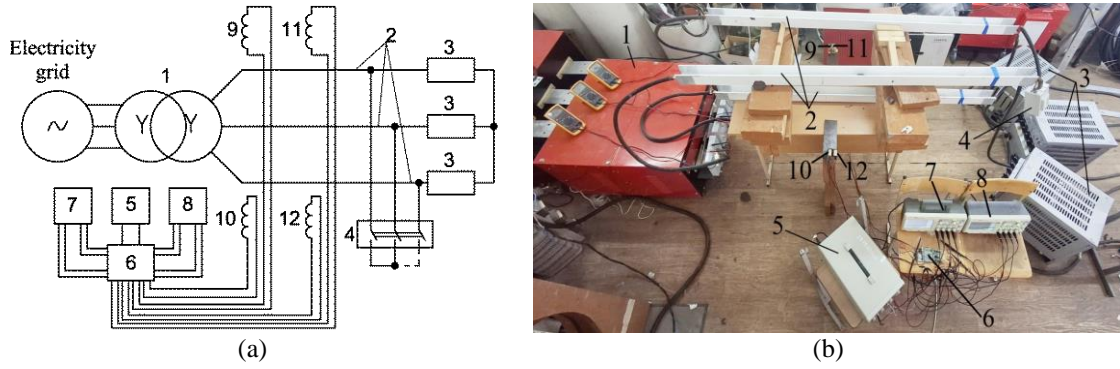


Figure 4. Laboratory setup (a) diagram and (b) assembly

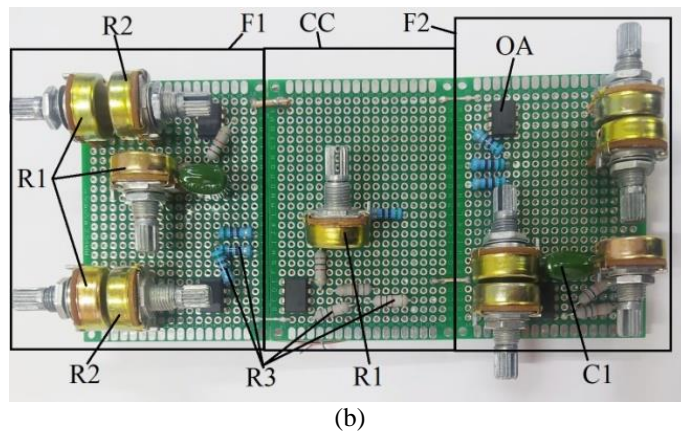
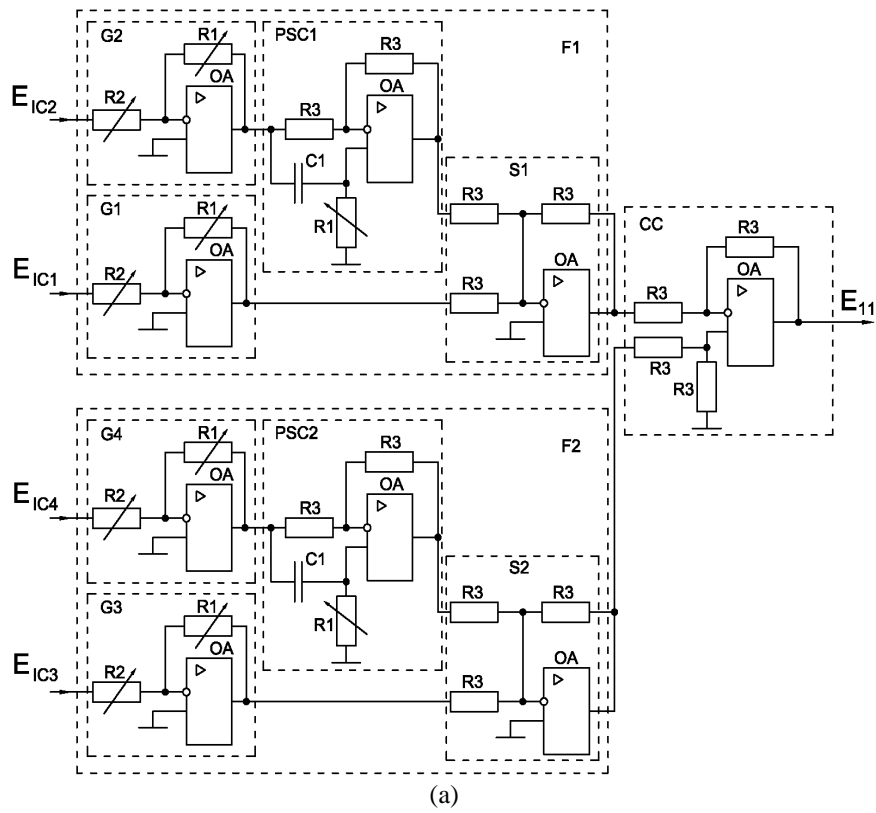


Figure 5. Laboratory prototype of the filter (a) circuit and (b) top view

### 3.3. Structure for fastening IC

A structure for fastening IC is shown in Figure 6 [34]. It includes bar "1" attached by clamp "2" to support "3"; plates "4"; casings "5" CIs are mounted inside; rods "6" and "7" with scales; beam "8"; fastening clips "9"; regular triangle "10" with bus ducts of phases A, B, and C attached to with insulators "11". Triangle 10 is attached to a cross arm (not shown in Figure 6). Beam 8 connects rod 7 and support 3 to ensure rigidity of the structure. The position of plates 4 is changed by moving them along rods 6 and 7. An IC is fixed inside casing 5 and can rotate and move in the cross-sectional plane of phases A, B, and C. The structure is simple, easy-to-handle, and is made of nonmagnetic materials; its weight with the IC (100 to 200 g) does not exceed 5 to 7 kg.

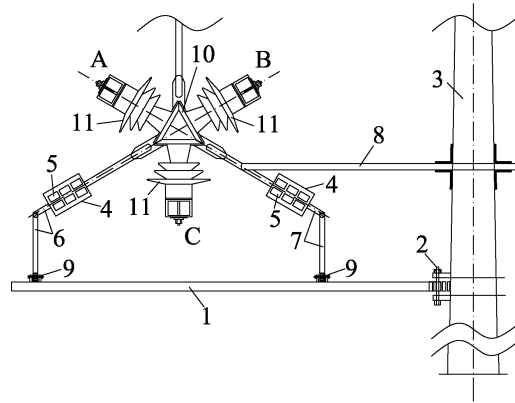


Figure 6. Structure for fastening IC near phase bus ducts

## 4. RESULTS AND DISCUSSION

### 4.1. Simulation results

Figure 7 shows oscillograms of voltages  $\underline{E}_{\Sigma 1}$  and  $\underline{E}_{\Sigma 2}$  at exits of filters F1 and F2;  $\underline{E}_5$  and  $\underline{E}_9$  after amplification (after amplifiers 5 and 9 in Figure 1 and after blocks "Gain 2" and "Gain 4" in Figure 3(b), and  $\underline{E}_{11}$  at the exit of block "Subtract" in Figure 3(b). Under the load mode,  $\underline{E}_{\Sigma 1} = \underline{E}_{imb1}^{load}$  and  $\underline{E}_{\Sigma 2} = \underline{E}_{imb2}^{load}$  ( $\underline{E}_{imb1}^{load}$  and  $\underline{E}_{imb2}^{load}$  are the imbalance voltages of filters F1 and F2 when the maximal load current flows in phases of the 100-kV line). In this case,  $|\underline{E}_{11}| < E_{op}$  and circuit 11 does not operate. In the event of a three-phase SC in Figure 7(a) in a steady state,  $\underline{E}_5$  and  $\underline{E}_9$  are opposite in phase; therefore,  $E_{\Sigma 1} = E_{imb1}^{(3)}$  and  $E_{\Sigma 2} = E_{imb2}^{(3)}$  ( $E_{imb1}^{(3)}$  and  $E_{imb2}^{(3)}$  are the imbalance EMF at terminals 18 and 19, 20 and 21 when three-phase SC currents flow in the busbars), and  $E_{imb1}^{(3)} > E_{imb1}^{load}$  and  $E_{imb2}^{(3)} > E_{imb2}^{load}$ . In a transient mode,  $\underline{E}_{\Sigma 1}$  and  $\underline{E}_{\Sigma 2}$  strongly increase and become commensurate with the EMF at the filter terminals during a two in Figure 7(b) and single-phase in Figure 7(c) short circuits, when negative-sequence currents appear. To avoid unnecessary operation of a protection device based on the suggested filter, a time delay should be introduced. During all SC types,  $|\underline{E}_{11}| > E_{op}$ . In the case of breaking cables from IC 1,  $|\underline{E}_{11}| > E_{op}$  and circuit 15 operates in Figure 7(d). Using a model, filter quality parameters characterizing were determined [26]: the conversion coefficient  $m = 1.6$  and the coefficient  $\gamma f = 0.11$  which characterizes a change in the imbalance value at the filter output when the network frequency deviates. Note that the coefficient  $m$  is the same as for filters with current transformers and those mentioned above [26]–[29], and the imbalance voltage stronger depends on a change in the network frequency (at  $f = 48\text{--}52$  Hz, the unbalance increases by 7%). For a microprocessor filter, this imbalance can be reduced by adjusting the voltages phase shift angles.

### 4.2. Experimental results

Figure 8 shows the oscillograms of voltages  $\underline{E}_{\Sigma 2}$ ,  $\underline{E}_5$ ,  $\underline{E}_9$ ,  $\underline{E}_{11}$ , and  $U_p$  recorded under different modes during our experiments. Under the load mode,  $\underline{E}_{\Sigma 2} = \underline{E}_{imb2}^{load}$  and  $\underline{E}_{11} = E_{imb}$ . In the case of a short circuit in Figures 8(a) to 8(c),  $\underline{E}_{\Sigma 2}$ ,  $\underline{E}_5$ ,  $\underline{E}_9$ , and  $\underline{E}_{11}$  increase. In a transient mode,  $\underline{E}_{\Sigma 2}$  during a three-phase SC is commensurate with the EMF during a two-phase SC and is much lower in the steady state;  $E_{11}$  are nearly equal in both modes. If a cable from IC 2 to amplifier 6 in Figure 8(d) breaks,  $\underline{E}_{11} > E_{imb}$ , and the output relay (not shown in Figure 5) of the comparison circuit ( $U_p \neq 0$ ) actuates. The analysis of Figure 8 shows the efficiency and correct operation of the suggested negative-sequence current filter in the events of short circuits and breaks in connecting conductors.



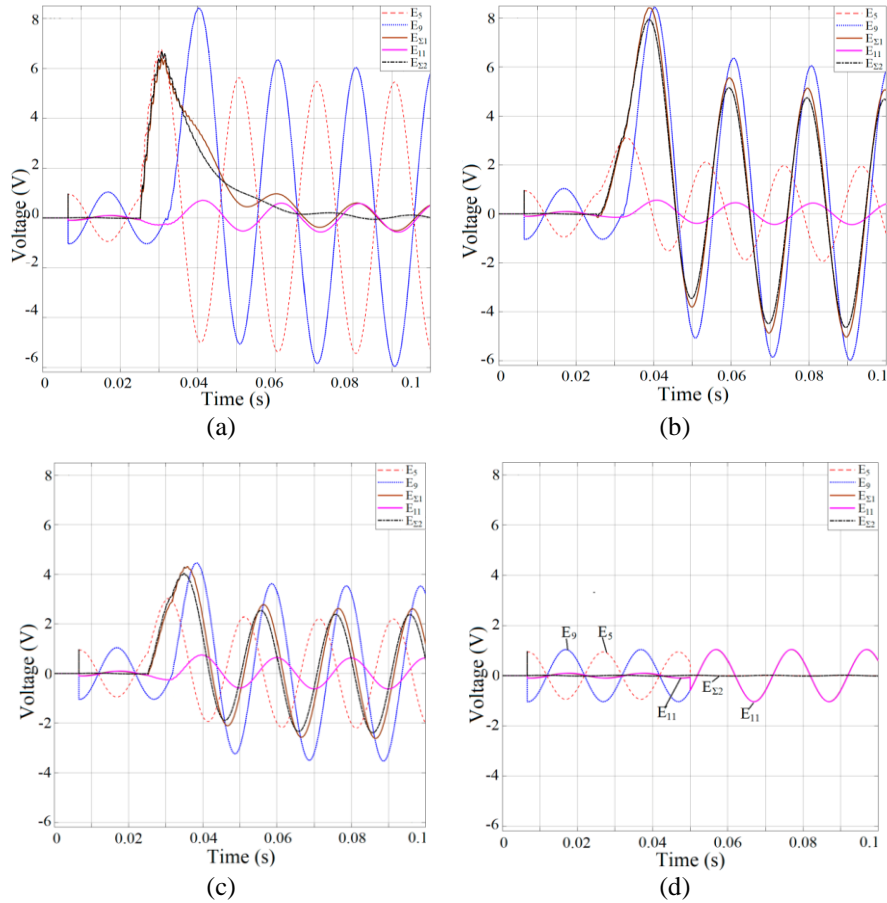


Figure 7. Oscillograms of EMF  $E_{\Sigma 1}$ ,  $E_{\Sigma 2}$ ,  $E_5$ ,  $E_9$ , and  $E_{11}$  in the case of (a), (b), (c) SC in the electrical installation and (d) faults in the filter

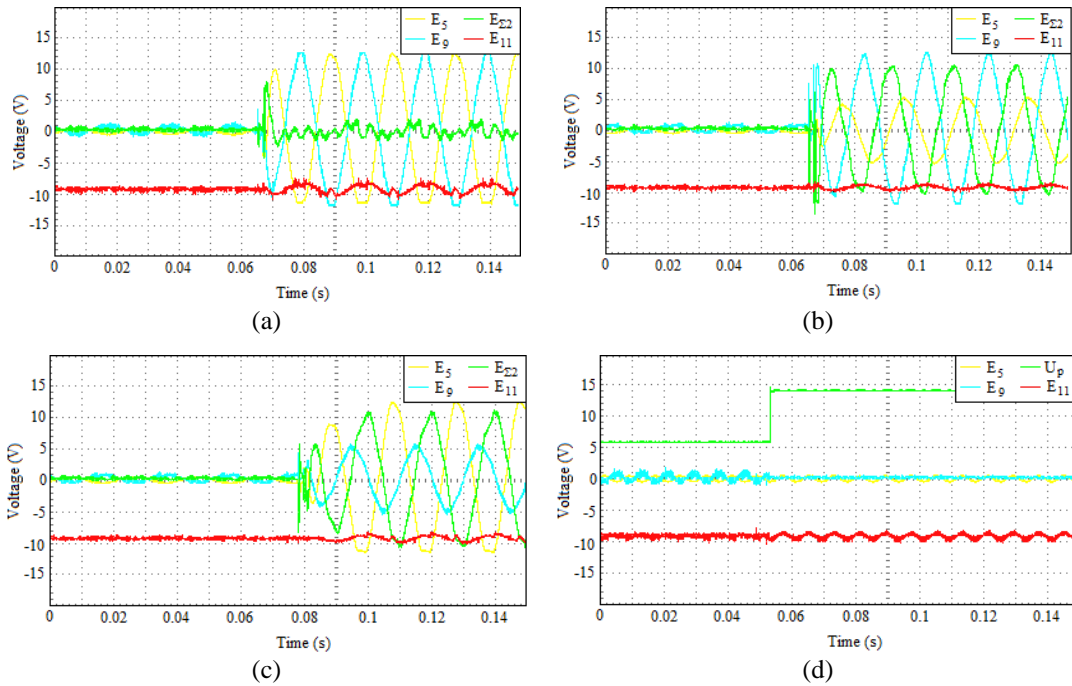


Figure 8. Oscillograms of voltages  $E_{\Sigma 2}$ ,  $E_5$ ,  $E_9$ , and  $E_{11}$  in the event of (a) three- and (b) and (c) two-phase SCs and (d) cable breaks

### 4.3. Discussion

#### 4.3.1. Novelty of the suggested solution

A negative-sequence current filter was designed. Its difference from the known ones [28]–[31] consists in the following: i) information about the current in an electrical installation is received from an inductance coil without using current transformers, a Rogowski coil, or a reed switch and ii) it has built-in functional diagnostics, which ensures real time detection of faults in the filter. Filter quality parameters (the coefficients  $m$  and  $\gamma f$ ) were determined. Methods for selecting filter parameters (amplifier gain and phase shift angle in the phase-rotation circuit) and determining the IC fixing points near the phase bus ducts (at the vertices of an equilateral triangle) were developed.

#### 4.3.2. Benefits of the research

The suggested filter is to enable building up highly sensitive filter protections of power transmission lines and current transformers (CTs) of 6 to 750 kV in voltage, enabling saving unprecedented amount of high-quality copper, steel, and high-voltage insulation (tens and hundreds of kilograms per connection). In terms of reliability, it should exceed both traditional protections and other mentioned protections due to duplication of IC and connecting cables and built-in fault diagnostics of filter components. Use of the filter as backup to traditional ones is to provide an increase in the reliability of a relay protection system as a whole, considering that current transformers will be duplicated, which are not duplicated now and introduce the main error in the filter operation due to saturation. There is no reason to doubt a possibility of building up similar filters in the case of other arrangement of phase bus ducts by analogy with the suggested method for filter designing and testing. Note that, unlike Rogowski coils and current transformers, mounting ICs at safe distances from phases allows their safe service even when an electrical installation is turned on.

#### 4.3.3. Limitations of the suggested technique for designing the filter

Protections based on the suggested filter should have a time lag longer than the duration of a transient process during a three-phase short circuit in order to prevent unnecessary operation. The transient process lasts no more than 0.03 s in simulation with a voltage of 110 kV and 4 ms in experiments at 0.4 kV. However, this time increases with voltage and upon changes the network configuration; therefore, the required time delay is unknown. The filter can only be used for single-standing electrical installations (for example, for a dead-end power transmission line). Another one disadvantage is a need in designing different structures for fastening ICs for electrical installations with a different arrangement of phase bus ducts.

#### 4.3.4. Future research directions

Future research directions include: i) Elimination of the above time lag; ii) Design of structures for fastening inductance coils of the filter for super-high voltage electrical installations and a different arrangement of phase bus ducts; and iii) Study of the filter behavior under interference from currents in adjacent electrical installations and ways of avoiding them.

## 5. CONCLUSION

The design of a negative-sequence current filter based on inductance coils for electrical installations with phase bus ducts located at the vertices of an equilateral triangle is suggested for the first time. This filter solves one of fundamentally unsolved problems in the electric power industry, *i.e.*, the problem of avoiding the use of current transformers. This filter being implemented is to enable saving high-quality copper, steel, and high-voltage insulation in amounts unprecedented for relay protection. We believe that the suggested filter will not be inferior to known filters in terms of all parameters except speed and will be superior in reliability due to the presence of functional diagnostics. The study of the filter behavior under different conditions (interphase and single-phase short circuits, load mode, failures of filter elements) in experiments and computer simulation confirmed the correctness of its operation. The filter design technique can be used to manufacture similar filters for electrical installations with any arrangement of phases.

## ACKNOWLEDGEMENTS




The work was supported by the Ministry of Science and Higher Education of the Republic of Kazakhstan (grant no. AP13268753).

## REFERENCES




- [1] F. A. Romaniuk, V. Y. Rumiantsev, and Y. V. Rumiantsev, "Symmetrical components digital filters for microprocessor-based protection input signals," *ENERGETIKA. Proceedings of CIS higher education institutions and power engineering associations*, vol. 66, no. 1, pp. 5–17, Feb. 2023, doi: 10.21122/1029-7448-2023-66-1-5-17.

- [2] Y. Bulatov, A. Kryukov, and K. Suslov, "Effect of unbalanced and non-linear loads on operation of the turbogenerator of a distributed generation unit." *Applied Sciences*, vol. 13, no. 6, Mar. 2023, doi: 10.3390/app13063643.
- [3] K. Solak, F. Mieske, and S. Schneider, "Negative-sequence current integral method for detection of turn-to-turn faults between two parallel conductors in power transformers," *International Journal of Electrical Power and Energy Systems*, vol. 141, Oct. 2022, doi: 10.1016/j.ijepes.2022.108124.
- [4] T. Liu, X. Zhao, J. Ma, S. Wang, Z. Wu, and R. Wang, "The current sequence components extraction for dual synchronous rotation frame current control in unbalanced grid conditions," *IEEE Journal of Emerging and Selected Topics in Power Electronics*, vol. 12, no. 2, pp. 1311–1323, Apr. 2024, doi: 10.1109/JESTPE.2023.3302914.
- [5] J. Yan *et al.*, "Overcurrent suppression method for multiple wind farms connected to MMC-HVDC," *IEEE Transactions on Circuits and Systems II: Express Briefs*, vol. 69, no. 11, pp. 4473–4477, Nov. 2022, doi: 10.1109/TCSII.2022.3185070.
- [6] G. E. Lint, *Symmetrical components in relay protection*, (in Russian), Energoatomisdat: Moscow, Russia, 1996. Accessed: Oct. 01, 2024. [Online]. Available: [https://archive.org/download/1996\\_20200728](https://archive.org/download/1996_20200728)
- [7] J. Das, *Power systems protective relaying*. 6000 Broken Sound Parkway NW, Suite 300, Boca Raton, FL 33487–2742: CRC Press, 2017.
- [8] M. K. (Mondal) and S. Debnath, "Fault location in UPFC compensated double circuit transmission line using negative sequence current phasors," *Electric Power Systems Research*, vol. 184, Jul. 2020, doi: 10.1016/j.epsr.2020.106347.
- [9] L. A. Kojovic, "Non-conventional instrument transformers for improved substation design," *CIGRE Session 46*, 2016.
- [10] M. Y. Kletsel, B. E. Mashrapov, and R. M. Mashrapova, "Reed switch protection of double-circuit lines without current and voltage transformers," *International Journal of Electrical Power and Energy Systems*, vol. 154, Dec. 2023, doi: 10.1016/j.ijepes.2023.109457.
- [11] V. E. Kazansky, *Measuring current transformers in relay protection*, (in Russian), Moscow, Russia: Energoatomisdat, 1988.
- [12] D. D. Issabekov, Z. B. Mussayev, V. P. Markovskiy, A. P. Kislov, and D. S. Urazalimova, "Reed switch overcurrent protection: new approach to design," *Energies*, vol. 17, no. 11, May 2024, doi: 10.3390/en17112481.
- [13] J.-H. Teng, S.-W. Luan, W.-H. Huang, D.-J. Lee, and Y.-F. Huang, "A cost-effective fault management system for distribution systems with distributed generators," *International Journal of Electrical Power and Energy Systems*, vol. 65, pp. 357–366, Feb. 2015, doi: 10.1016/j.ijepes.2014.10.029.
- [14] V. Gurevich, *Electric relays: principles and applications*. CRC Press, 2018.
- [15] V. Goryunov, M. Kletsel, B. Mashrapov, Z. Mussayev, and O. Talipov, "Resource-saving current protections for electrical installations with isolated phase busducts," *Alexandria Engineering Journal*, vol. 61, no. 8, pp. 6061–6069, 2022, doi: 10.1016/j.aej.2021.11.031.
- [16] A. Neftissov, A. Biloshchytskyi, O. Talipov, and O. Andreyeva, "Determination of the magnitude of short-circuit surge current for the construction of relay protection on reed switches and microprocessors," *Eastern-European Journal of Enterprise Technologies*, vol. 6, no. 5 (114), pp. 41–48, Dec. 2021, doi: 10.15587/1729-4061.2021.245644.
- [17] D. G. Pellinen, M. S. Di Capua, S. E. Sampayan, H. Gerbracht, and M. Wang, "Rogowski coil for measuring fast, high-level pulsed currents," *Review of Scientific Instruments*, vol. 51, no. 11, pp. 1535–1540, Nov. 1980, doi: 10.1063/1.1136119.
- [18] L. A. Kojovic, M. T. Bishop, and D. Sharma, "Innovative differential protection of power transformers using low-energy current sensors," *IEEE Transactions on Industry Applications*, vol. 49, no. 5, pp. 1971–1978, Sep. 2013, doi: 10.1109/TIA.2013.2264792.
- [19] M. Habrych, G. Wisniewski, B. Miedzinski, A. Lisowiec, and Z. Fjalkowski, "HDI PCB Rogowski coils for automated electrical power system applications," *IEEE Transactions on Power Delivery*, vol. 33, no. 4, pp. 1536–1544, Aug. 2018, doi: 10.1109/TPWRD.2017.2765400.
- [20] B. Li, M. Wen, X. Shi, L. Wang, and Y. Chen, "An improved fast distance relay to mitigate the impacts of Rogowski coil transducer transient," *IEEE Transactions on Power Delivery*, vol. 37, no. 3, pp. 1549–1558, Jun. 2022, doi: 10.1109/TPWRD.2021.3092427.
- [21] E. M. Esmail, A. Almalaq, K. Alqunun, Z. M. Ali, and S. H. E. A. Aleem, "Rogowski coil-based autonomous fault management strategy using Karen Bell transformation for earthed active distribution networks," *Ain Shams Engineering Journal*, vol. 14, no. 5, May 2023, doi: 10.1016/j.asej.2022.101953.
- [22] A. N. Sarwade, M. M. Jadhav, and S. P. Patil, "Transmission line fault analysis using ANN and Rogowski coil," *International Journal of Advanced Technology and Engineering Exploration*, vol. 10, no. 99, Feb. 2023, doi: 10.19101/IJATEE.2021.876104.
- [23] S. Ranasingh, T. Pradhan, D. K. Raju, A. R. Singh, and A. Piantini, "An approach to wire-wound hall-effect based current sensor for offset reduction," *IEEE Sensors Journal*, vol. 22, no. 3, pp. 2006–2015, 2022, doi: 10.1109/JSEN.2021.3133105.
- [24] M. Crescentini, S. F. Syeda, and G. P. Gibiino, "Hall-effect current sensors: Principles of operation and implementation techniques," *IEEE Sensors Journal*, vol. 22, no. 11, pp. 10137–10151, Jun. 2022, doi: 10.1109/JSEN.2021.3119766.
- [25] R. Majumder, S. Dolui, D. Agasti, and S. Biswas, "Micro-controller based over current relay using Hall Effect current sensor," in *2018 Emerging Trends in Electronic Devices and Computational Techniques (EDCT)*, Mar. 2018, pp. 1–4, doi: 10.1109/EDCT.2018.8405086.
- [26] K.-L. Chen, R.-S. Wan, Y. Guo, N. Chen, and W.-J. Lee, "A redundancy mechanism design for hall-based electronic current transformer," *Energies*, vol. 10, no. 3, Mar. 2017, doi: 10.3390/en10030312.
- [27] I. M. Sirotka and I. M. Shurin, *Phase sequence network in circuits with remote sensors*, (in Russian), no. 11. *Electrichestvo*, 1971. Accessed: Oct. 01, 2024, [Online]. Available: <https://www.booksite.ru/elektr/1971.htm>
- [28] D. B. Solovev and A. S. Shadrin, "Instrument current transducers with Rogowski coils in protective relaying applications," *International Journal of Electrical Power and Energy Systems*, vol. 73, pp. 107–113, 2015, doi: 10.1016/j.ijepes.2015.04.011.
- [29] D. B. Solovev and A. S. Shadrin, "Instrument current transducer for measurements in asymmetrical conditions in three-phase circuits with upper harmonics," *International Journal of Electrical Power and Energy Systems*, vol. 84, pp. 195–201, Jan. 2017, doi: 10.1016/j.ijepes.2016.05.012.
- [30] M. Kletsel, A. Zhantlesova, P. Mayshev, B. Mashrapov, and D. Issabekov, "New filters for symmetrical current components," *International Journal of Electrical Power and Energy Systems*, vol. 101, pp. 85–91, Oct. 2018, doi: 10.1016/j.ijepes.2018.03.005.
- [31] B. Issabekova, M. Tokombaev, and A. Zhantlessova, "Reed switch protection devices with symmetric component filter without current transformers," in *2021 International Ural Conference on Electrical Power Engineering (UralCon)*, Sep. 2021, pp. 141–146, doi: 10.1109/UralCon52005.2021.9559592.
- [32] K. M. Yakovlevich, M. B. Yerbolovich, and M. G. Narimanovna, "Negative sequence current filter for electrical installations with phase conductors located at the vertices of an equilateral triangle," (in Tajik), KZ Patent 36286, 2022/0285.1, 2023. Accessed: Oct. 01, 2024. [Online]. Available: <https://gosreestr.kazpatent.kz/Invention/Details?docNumber=357371>
- [33] V. K. Vanin and G. M. Pavlov, *Relay protection on computing elements*, (in Russian), Ed. 2. Leningrad, Russia: Energoatomisdat, 1991. Accessed: Oct. 01, 2024, [Online]. Available: <https://f.eruditor.link/file/1109883/>
- [34] K. M. Yakovlevich, A. B. Zhantlesova, B. B. Zhantlesova, and N. T. Yerzhanov, "Structures for fastening and controlling parameters of microcontrollers for three-phase symmetrical bus ducts of 1–10 kV in voltage," KZ Patent 20265, 2006.




**BIOGRAPHIES OF AUTHORS**

**Mark Kletsel**    received the Doctor of Technical Sciences degree in electrical power engineering from Kazakh Scientific Research Institute of Power, Kazakhstan, in 1998. Currently, he is a professor at the Department of Electric Power Industry, Toraighyrov University. He has authored or coauthored more than 300 refereed journal and conference papers. His research interests include power transmission reliability, relay protection, power transmission protection, overcurrent protection, and power distribution protection. He is a reviewer for journals computers and electrical engineering and sustainable energy, grids and networks. He can be contacted at email: mkletsel@mail.ru.






**Bauyrzhan Mashrapov**    received the B.Sc., M.Sc., and the Ph.D. degree in electrical power engineering from Toraighyrov University, Kazakhstan, in 2009, 2011, and 2014, respectively. Currently, he is an associate professor at the Department of Electric Power Industry, Toraighyrov University. He has authored or coauthored 50 refereed journal and conference papers. His research interests include relay protection, power transmission protection, overcurrent protection, and power distribution protection. He can be contacted at email: bokamashrapov@mail.ru.



**Rizagul Mashrapova**    received the B.Sc., M.Sc., and the Ph.D. degree in electrical power engineering from Toraighyrov University, Kazakhstan, in 2009, 2011 and 2021, respectively. Currently, he is an associate professor at the Department of Electric Power Industry, Toraighyrov University. His research interests include relay protection, power transmission protection, overcurrent protection, and power distribution protection. He can be contacted at email: rizka1504@mail.ru.



**Alexandr Kislov**    has graduated from the Faculty of Energy Engineering of Pavlodar Industrial Institute. He defended his candidate's dissertation at Moscow Energy Engineering Institute in 1987. Currently, he is a professor at the Department of Electrical Engineering and Automation, Toraighyrov University. He is also a full member of the International Informatization Academy. He has authored or coauthored more than 100 refereed journal and conference papers. He can be contacted at email: kislovpsu@mail.ru.